Atomistic Modeling for 3D Dynamic Simulation of Ion implantation into Crystalline Silicon

Myung-Sik Son*, Jeong-Won Kang*, Ki-Ryang Byun*, and Ho-Jung Hwang*
*Semiconductor Process and Device Lab, Dept. of Electronic Engineering,
Chung-Ang University, Seoul, 156-756, Korea
Tel: 82-2-820-5296 Fax: 82-2-825-1584 E-mail: sms@semilab3.ee.cau.ac.kr

Abstract - In this paper are presented a newly proposed 3D Monte Carlo (MC) damage model for the dynamic simulation in order to more accurately and consistently predict the implant-induced point defect distributions of the various ions in crystalline silicon. This model was applied to Phosphorus implants for the ULSI CMOS technology development. In addition, a newly applied 3D-trajectory split method has been implemented into our model to reduce the statistical fluctuations of the implanted impurity and the defect profiles in the relatively large implanted area as compared to 1D or 2D simulations. Also, an empirical electronic energy loss model is proposed for Phosphorus and Silicon implants. The 3D formations of the amorphous region and the ultra-shallow junction around the implanted region could be predicted by using our model, TRICSI(TRansport Ions into Crystal-Silicon).

Introduction

The continued scaling of feature size in the ULSI device technology has required shallower, more compact impurity profiles, and more precisely controlled doping profiles. In addition, the implant-induced damage has large effect on the impurity diffusion such as TED (Transient Enhanced Diffusion) phenomena during thermal annealing after ion implantation. Detailed understanding is needed of dependence of both the impurity and the damage profiles on all of the key implant parameters such as energy, dose, tilt and rotation of the wafer. Simulation of subsequent thermal processing (diffusion models) must begin with the correct as-implanted impurity and the damage profiles. As a result, greatly reduced thermal budgets are necessary for the development and manufacturing of ULSI CMOS devices. For this reason, the final dopant profile after heat treatments depends more strongly on the as-implanted impurity and the defect profiles, and an accurate and efficient physically-based 3D model capable of predicting the as-implanted dopant and the defect profiles around and under the implanted area becomes highly desirable.

In this paper are presented a newly proposed 3D Monte Carlo (MC) damage model for the dynamic simulation in order to more accurately and consistently predict the implant-induced point defect distributions of the various ions in crystalline silicon. This model was applied to P implants for the ULSI CMOS technology development. In addition, a newly applied 3D-trajectory split method has been implemented into our model to reduce the statistical fluctuations of the implanted impurity and the defect profiles in the relatively large implanted area as compared to 1D or 2D simulations. Also, an empirical electronic energy loss model is proposed for Phosphorus and Silicon implants. The 3D formations of the amorphous region and the ultra-shallow junction around the implanted region could be predicted by using our model, TRICSI (TRansport Ions into Crystal-Silicon).

Electronic Energy Loss (EEL) Model

It consists of nonlocal part (nonlocal model) that is proportional to the flight-path length Ls, and an impact parameter dependent part (local model) similar to the Hobler's Model [*Hobler et. al Nucl.Inst.Meth.B96 (1995) 155-162*]. Our difference exists in the local model. The local model is used the modified Firsov Model [*S.J. Morris et. al IEDM96 (1996) 721 723*] instead of the Oen-Robin model. For the P and Si, the screening length a was used 0.58 times the Moliere screening length a_m. The ratio of the local part to the nonlocal part was set to $(1 - 0.25(E/eV)^{0.05})$ to $(0.25(E/eV)^{0.05})$ for our simulations, in which E denotes the energy in eV unit. The correction factor k/k_L to the Lindhard model was set to 1.55. Our model shows very good agreements with the previously published data over the energy range from 10 to 180 keV.

Atomistic Modeling for 3D Dynamic Simulation

(i) Due to the forwarding momentum transfer of moving ion into silicon bulk to the lattice silicon, the recoiled silicon is more directed into silicon substrate. For this reason, the interstitial (I) and the vacancy (V) distribution is different from each other to and pro the damage peak range [*Ziegler, Handbook of ION IMPLANTATION TECHNOLOGY, North-Holand, 1992*]. Therefore, the trajectories of both implanted ions and recoiled silicons are directly followed to more accurately

predict the 3D distributions of both the quantitative point defects and the dopants depending on these phenomena.

(ii) For the computationally efficient dynamic simulation in the relatively large implanted area compared to 1D or 2D simulation, the channeling, dechanneling and rechanneling processes of the moving atoms and the spontaneous ***in situ*** annealing between I and V should be included. We separately treated each information of the numbers of both vacancies and interstitials saved at each unit volume $\Delta x\Delta y\Delta z$ according to their stopped, annihilated, and generated positions. With the statistical information of the point defects, the damaged silicon structures are modeled using the vacancy probability for vacancy creation and the dechanneling damage probability to affect the motions of both the implanted ions and the recoiled silicons. Instead of choosing the tetrahedral sites as an interstitial site [*K.M. Klein et. al., Nucl. Inst. Meth. B59/60 (1991) 60*], we used the random interstitial sites and the vacancy sites at the silicon lattice sites.

(iii) The following descriptions are for the dynamic simulation procedures: The FPLS (the flight-path length between two collision atoms in the ideal crystal structure) is first searched in the crystal structure, which has no damage. After that, the number of interstitials and vacancies are counted in the one or extended local unit volumes, which might has more than two unit volumes added and should include the FPLS path in the nearest cubics. And then, the interstitials are created and the interstitial hit collision occurred according to the following formula (1) if the random number Rn evenly distributed between 0 and 1 is content with the condition of the below equation:

$$Rn < Pint(x,y,z) = Nint/(k \cdot Nsat) \quad (1)$$

The k factor was set to 0.5 for modeling the interstitial clusters or amorphous pockets. This is from the fact the point defects exists more cluster-like defects from the result of the MD (molecular dynamic) simulation. The weight factor of vacancy increment for the silicon recoil is Wion. The Wion is the weight factor of one pseudoparticle defined as the equation of (Implanted Area [cm] $\cdot$Dose[ions/cm^2] / $\Delta x\Delta y\Delta z$ [cm^3]) $\cdot$(1 / Total Simulated Ions). In addition, the weight factor of interstitial decrement for the self-interstitial recoil is set to the same Wion. If the moving motions for ion and recoils are stopped, the same increments with the above described weight factor for vacancy and interstitial are added if the recombination with the counterpart is not occurred. The interstitial position is determined on the FPLS line to the 3D moving direction of the ion and recoiled silicon by the following formula:

$$Ls = (FPLS - Rcap) \cdot Rn + Rcap \quad (2).$$

The Rcap [*K.M.Klein et. al., Nucl. Inst. Meth. B59/60 (1991)60*] is the capture radius for the vacancy-interstitial recombination. After failing in searching the interstitial described above, it is checked for the vacancy generation whether this collision silicon position in the ideal crystal structure is occupied by a vacancy. The following condition is used:

$$Rn < Pvac(x,y,z) = Nvac / Nsi \quad (3)$$

,where the silicon density Nsi is $9.4725 \times 10^{21}/cm^3$.

The above sequence for each collision step with the interstitial or the stationary silicon or the vacancy is repeated until the local region is completely amorphized. After the region is amorphized, the amorphous TRIM [*J.F. Ziegler, J.P. Biersack, The stopping and Range of Ions in Solids, Vol. I, New York : Pergamon(1985)*] model is used. The amorphous criteria in the local volume is defined as the total point defect concentration of Nvac+Nint is reached to and over the saturation concentration Nsat of the point defect, which is determined by the capture radius Rcap for the interstitial-vacancy recombination. We used 0.54 times the silicon lattice constant of 5.43095Å for the Phosphorus implants. The Nsat is about 20 % of the silicon density Nsi, that is, 1E22/cm^3.

(iv) The ***in situ*** annealing of the defect recombination during ion implantation at room temperature is considered, which resulted in the saturation concentration of Nsat for the point defect. We defined the interstitial recombination probability based on the counterpart vacancy concentration:

$$Precint(x,y,z) = Nvac / Nsat \quad (4)$$

at each interstitial generation. The vacancy recombination probability based on the concentration of the interstitial:

$$Precvac(x,y,z) = Nint / Nsat \quad (5)$$

at each vacancy generation, where the Nvac and Nint is the safely existed interstitial and the previously created vacancy concentrations in the local volume, respectively. The following conditions of (4) and (5) equations are used for checking the defect recombination at each defect generation: For each vacancy generation, generating the random number in the following equation checks the recombination condition with the previously existed interstitials:

$$Rn < Precvac(x,y,z) \quad (6).$$

For each interstitial generation, generating the random number in the following equation checks the recombination condition with the previously existed vacancies:

$$Rn < Precint(x,y,z) \quad (7)$$

The decrement quantity of each interstitial and vacancy is the same with the counterpart weight factor described above as increment for vacancy or decrement for interstitial.

Self-Adaptive Modeling for 3D Virtual Trajectory Split

In order to reduce the statistical fluctuations in the 3D distributions of both the impurity and the defect due to the lack of the simulated particles in the large area, the trajectory split method are three-dimensionally applied in our dynamic damage model. Our simple approach for the trajectory split method is similar to that of the UT-MARLOWE [*S.-H. Yang et. al, The Electrochemical Society Proceeding of Process Physics and Modeling in Semiconductor Technology (1996), PV'96-4, pp.481*]. The different virtual split criteria are used and the split-levels based on the range profile are extended to two lateral directions. In our technique, in the Region I only for the 1D application several, the same distances for depth D_1, D_2,..., D_n to the X depth direction are located.

In the Region II deviated regions from each mask edge to both two lateral directions from the, not the volume under the implanted square window, the lateral same distances L_1, L_2, ... , L_n from each mask edge is located. The n of the total number of levels for splitting the ions is 10 used. The lateral equi-distance is the same distance to two lateral directions and used by half of the distance of a depth level. For the lateral splits of moving ions, the entering point into silicon bulk is set to a first line. From the line, the lateral split lines are located to two lateral directions. And so, we can consider the mask structure for splits.

The full-dynamic simulation on each virtual split branches is made in the sequence of the above described dynamic damage model. And also, all of the recoiled silicons made by the split branches are explicitly followed. Therefore, the fluctuation of the defect distribution is more reduced as shown in Fig.2.

Simulation Results and Conclusions

Our model explicitly takes into account the generation and recombination of point defects, the amorphization of the crystal silicon, and the channel blocking by the implant-induced damage. The new full-dynamic damage model predicts well the impurity range profile dependence on the dose, energy and tilt conditions for the P implants into (100) crystal silicon as shown in Fig. 1a, 1b, 1c, 1d. The 10 and 20 keV SIMS data in Fig. 1d are from Samsung Electronics Company, Korea.

In our results for point defects, the point defect distributions are much less than those of the modified Kinchin-Pease approach over commonly used energy range from 10 and 180 keV. We found that the reduction factor due to self-anneal for the result of the Kinchin-Pease approach fitted to our results is about 0.45 times the Kinchin-Pease Calculation.

In the cases at and below 30 keV, the vacancy distributions are less than the interstitial distributions from the surface to about 100 Å. This discrepancy is from the fact that the recoiled silicons are out of surface to reduce the interstitials from the surface below 100A region. However, in other cases over 30 keV, the vacancy and the interstitial distributions are less different in the 1D results. Therefore, high-energy cases over 30 keV in our simulations do not show the different profiles for each vacancy and interstitial over 1D distribution. But, this discrepancy increases in the low-energy case as shown in Fig.1d. We show the 3D damage range profiles and each vacancy and interstitial profile at 30 keV, 7-degree tilt to the left in the figure and high-dose case. These results show the recoiled self-interstitials are more directed into the bulk as the vacancies left behind. The overall defect range profiles over 10 to 180 keV resembles the P-implanted range profiles and the damage peak is just before the ion peak, that is, near to the surface.

The 3D dopant range profile and 3D formations of the amorphous region and the ultra-shallow junction for the ULSI device technology could be predicted using our model as shown in Fig.2a and 2b. Our quantitative damage information in Fig. 1b and 2 could be presented to next thermal process simulations such as TED.

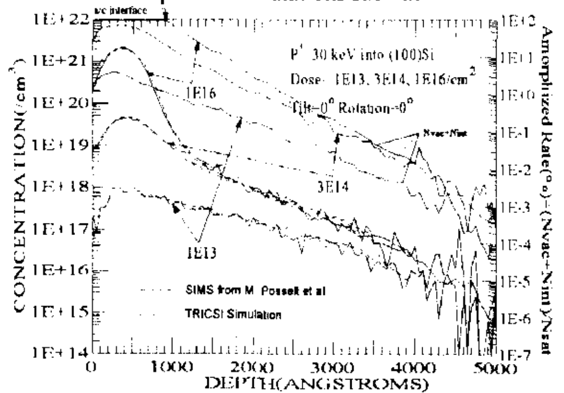

(a) Energy 30 keV, Dose 1E13, 3E14, and 1E16/cm², Tilt 0° and Rotation 0°

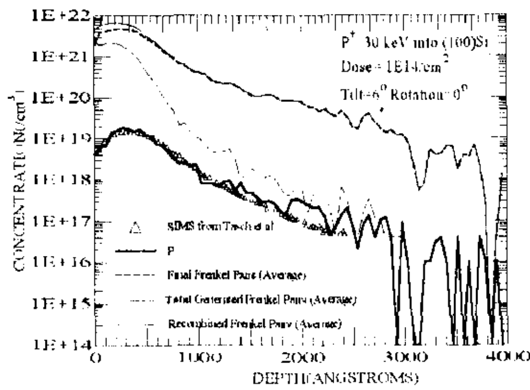

(b) Energy 30 keV, Dose 3E14, Tilt 7° and Rotation 0°

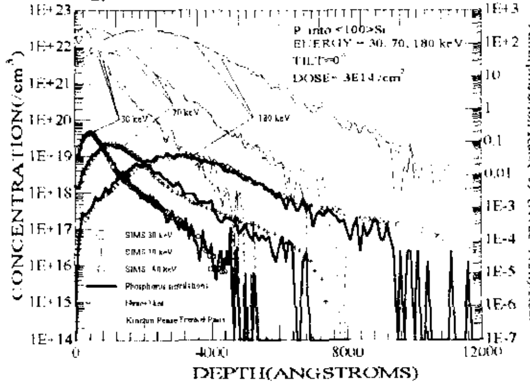

(c) Energy 30, 70 and 180 keV, Dose 3E14, Tilt 0° and Rotation 0°

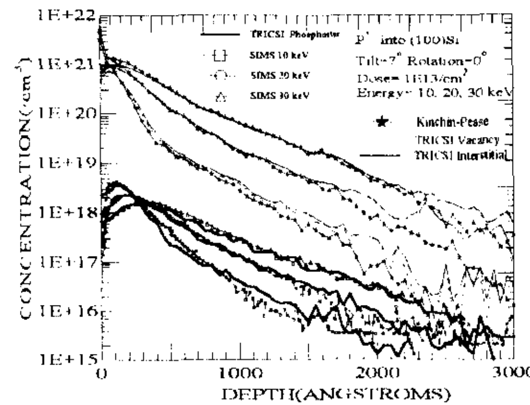

(d) Energy 10, 20, and 30 keV, Dose 1E13, Tilt 7° and Rotation 0°.

Fig.1 Simulation results of 1D P-implanted range and point defect concentration profiles with the 1D SIMS data, where the amorphized rate (%) is defined as (Nvac+Nint) / Nsat: In Fig. 1(a), we showed the 1D amorphized thickness measured by XTEM from M. Posselt et.al*[J. of Electrochemical Society, 144(4), pp. 1495, 1997]*, for comparison with our calculation. The super-particle approach has been used for the results in 2a, 2c, 2d, and the real ion approach for the results in 2b

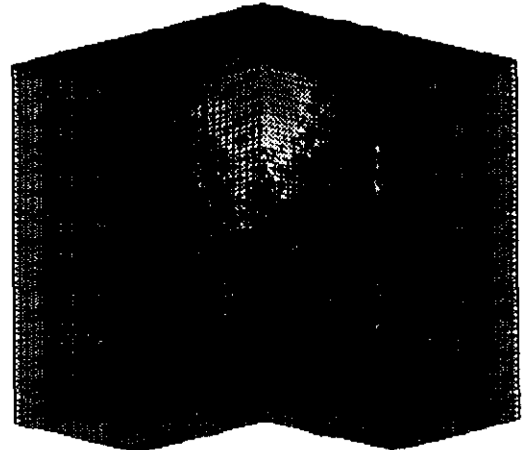

(a) 1/4 sected 3D Phosphorus profile

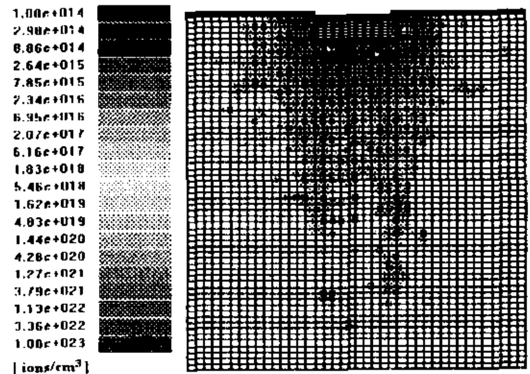

(b) Amorphized regions indicated by white circles on 2D section view

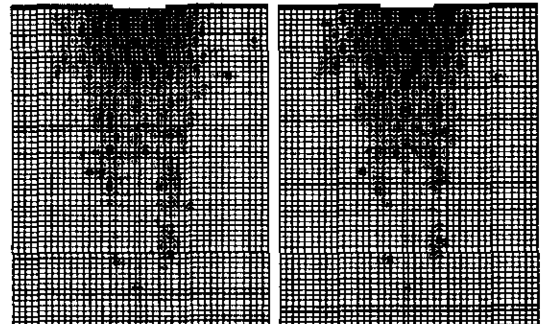

(c) 2D Interstitial Profile (d) 2D Vacancy Profile

Fig.2 3D Phosphorus range profile and implant-induced interstitial and vacancy concentration profiles at 30 keV, dose 1E16/cm^2, tilt 7° and rotation 0°. The split branches were 3, split lines were 6 and simulation particles were 5,000 ions. The mesh volume is used 10 × 10 × 10 nm^3. The implant open area is 100 × 100 nm^2. The implanted volume is 400 × 400 × 600 nm^3.